W boson loop background to $H \rightarrow ZZ$ at photon-photon colliders

M. S. Berger
Physics Department, University of Wisconsin, Madison, Wisconsin 53706
(Received 19 July 1993)

We have performed a complete one-loop calculation of $\gamma\gamma \rightarrow ZZ$ in the standard model, including both gauge bosons and fermions in the loop. We confirm the large irreducible continuum background from the W boson loop found by Jikia. We have included the photon-photon luminosity, and find that the continuum background of transverse Z boson pairs prohibits finding a heavy Higgs boson with a mass $\gtrsim 350$ GeV in this decay mode.

PACS number(s): 14.80.Gt, 14.80.Er

I. INTRODUCTION

The search for the mechanism of electroweak symmetry breaking is one of the most important challenges facing particle physics today. Detailed studies of the feasibility of the signal for Higgs bosons have been undertaken in this area for both hadron and e^+e^- colliders. The possibility of creating a photon-photon collider by Compton backscattering laser beams off electron beams has attracted much attention recently. These machines would provide collisions of photons at energies almost as high as the parent e^+e^- colliders, leading to recent interest in the possibility of detecting Higgs bosons at photon-photon colliders [1–3]. This also offers the possibility that the Higgs-boson–photon–photon coupling can be measured, and so provides an indirect probe of new physics because of any new charged particle that couples to the Higgs boson will contribute. New states contribute to the process $\gamma\gamma \rightarrow ZZ$ in the large energy region, $\sqrt{s_{\gamma\gamma}} \gg M_W$, as well [4]. While the photon-photon luminosity via the Weizsacker-Williams spectrum falls rapidly with increasing diphoton mass, the possibility of using backscattered laser beams provides a flat luminosity or even a luminosity which grows with energy almost all the way to the energy of the parent e^+e^- collider.

The W loop contribution to $\gamma\gamma \rightarrow ZZ$ have been calculated recently in a nonlinear gauge by Jikia [5] who found a large cross section for transverse Z's. We have performed an independent calculation of this process in the Feynman gauge (R_ξ with $\xi = 1$). We find a total cross section as well as contributions from individual helicity modes to be in good numerical agreement with the results of Jikia. We are also in good numerical and analytic agreement with Glover and van der Bij who have calculated and published the matrix elements for $gg \rightarrow ZZ$ [6]. This result can be immediately translated into the fermion loop contribution for $\gamma\gamma \rightarrow ZZ$ with the appropriate coupling replacements for the quarks and including the charged leptons.

Most studies of Higgs detection at photon-photon colliders have neglected the irreducible continuum background of Z pairs that arise from W boson and fermion loops. The signal obtains its largest contribution from W loops, and the explicit calculation of the continuum background presented here and in Ref. [5] indicates that the contribution to the background from almost all the helicity modes is dominated by the W boson loops as well.

The calculation required is straightforward but very lengthy. There are 188 one-loop diagrams with W-boson loops in the R_ξ gauge. These are shown in Fig. 1; the mixed coupling between the photon, the charged Goldstone boson, and the W boson is present in this gauge. The Higgs pole appears in the diagrams in Fig. 1(b). We have performed the calculation with the symbolic manipulation programs FORM and MATHEMATICA using the tensor integral reduction algorithm of van Oldenborgh and Vermaseren [7]. We obtain analytic expressions for each helicity amplitude, offering the possibility of includ-

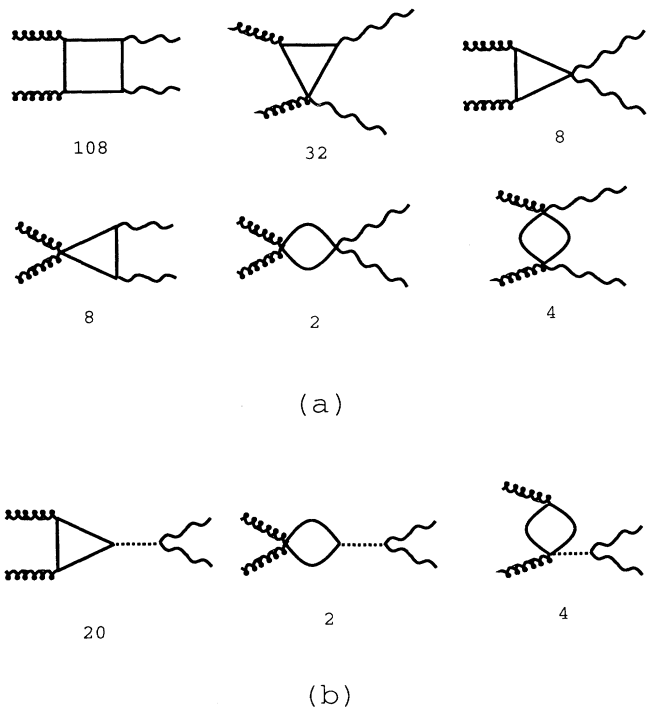

FIG. 1. Generic diagrams in the W boson loop contribution to $\gamma\gamma \rightarrow ZZ$. The loops consist of all possible combinations of W bosons, Goldstone bosons and ghosts, and the number of nonzero diagrams in each class (in a linear R_ξ gauge) is indicated. The dashed line is the Higgs boson.

ing the full spin correlations of the decay products of the Z bosons as well as arbitrary polarization of the incident photon beams. The result was derived for on-shell Z bosons, so it can be used for any energy above threshold $\sqrt{s_{\gamma\gamma}} > 2M_Z$. Jikia presented the cross sections for producing transverse and longitudinal Z bosons. In this paper we present the cross sections of each helicity mode of the Z's separately. We have investigated the feasibility of detecting a heavy Higgs boson at a photon-photon collider by convoluting the cross section with a realistic photon-photon luminosity from backscattering laser beams. We present cross sections for the Higgs signal and the continuum background. We have assumed a top quark mass of 150 GeV throughout this paper.

II. HELICITY AMPLITUDES AND CROSS SECTIONS

There are twelve independent cross sections. The contribution to the total cross section from each helicity amplitude will be denoted $\sigma_{\lambda_1\lambda_2\lambda_3\lambda_4}$ where λ_1 and λ_2 are the helicities of the photons and λ_3 and λ_4 are the helicities of the Z bosons. The cross sections for the helicity amplitudes with equal photon helicities are shown in Figs. 2(a), 2(b), and 2(c) for Higgs-boson masses of $M_H = 300$, 500, and 800 GeV, respectively. Only three of the amplitudes $(++++, ++--, +-+0)$ receive a contribution from the Higgs pole. The peaks for the heavier Higgs bosons are not as pronounced as the ones in Ref. [5] since we are using a top quark mass of 150 GeV rather than 120 GeV for which the destructive interference between the W boson loops and the top quark loops to the Higgs peak is more severe. The other amplitudes are independent of the Higgs-boson mass. There is interference between the Higgs pole and the continuum background that is constructive below the Higgs peak and destructive above.

The cross sections for the helicity amplitudes with unequal photon helicities is shown in Figs. 2(d). The contributions from the other helicity modes to the cross section are related by

$$\sigma_{+++-} = \sigma_{++-+} , \tag{1}$$

$$\sigma_{+-++} = \sigma_{+---} , \tag{2}$$

$$\sigma_{+++0} = \sigma_{++0+} , \tag{3}$$

$$\sigma_{++-0} = \sigma_{++0-} , \tag{4}$$

$$\sigma_{+-+0} = \sigma_{+-0-} , \tag{5}$$

$$\sigma_{+-0+} = \sigma_{+--0} . \tag{6}$$

The amplitudes $\mathcal{M}_{+-+-}$ and $\mathcal{M}_{+--+}$ are related by a crossing relation. A similar statement applies to $\mathcal{M}_{+-+0}$ and $\mathcal{M}_{+--0}$. The large cross section from the W boson loop arises in the helicity modes σ_{++++}, σ_{+-+-}, and σ_{+--+}. These contributions reproduce the large cross sections for transverse Z pairs at large $\sqrt{s_{\gamma\gamma}}$ first found by Jikia. For equal photon helicities the total cross section is dominated by σ_{++++} in the large energy domain. Likewise, the asymptotic value for the cross section in the case of opposite photon helicities is given by the sum of σ_{+-+-} and σ_{+--+}. These are the same helicity amplitudes that dominate the tree-level scattering $\gamma\gamma \to W_T^+ W_T^-$ [8]. The amplitudes $\mathcal{M}_{++++}$, $\mathcal{M}_{+-+-}$, and $\mathcal{M}_{+--+}$ are large because they grow logarithmically

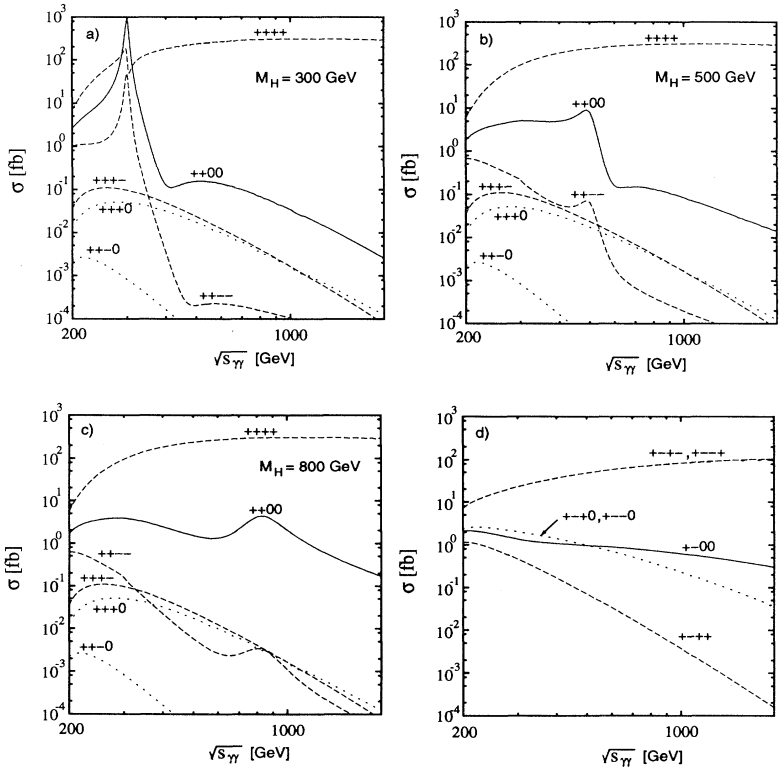

FIG. 2. The cross sections for each independent helicity amplitude is shown versus the diphoton mass, $\sqrt{s_{\gamma\gamma}}$. For photons with equal helicities the Higgs-boson mass is $M_H =$ (a) 300 GeV, (b) 500 GeV, and (c) 800 GeV. Cross sections for $Z_L Z_L$, $Z_T Z_L$, and $Z_T Z_T$ are shown with solid, dotted, and dashed lines, respectively. The top quark mass is taken to be 150 GeV.

with energy even at fixed scattering angle. This is unlike the contribution from fermion loops which approaches a constant at fixed scattering angle. For example, the largest helicity amplitude $\mathcal{M}_{++++}$ is given asymptotically ($\sqrt{s_{\gamma\gamma}} \gg M_W$) by

$$\mathcal{M}_{++++} = 8e^2 g^2 \cos^2\theta_W s_{\gamma\gamma}^2 [D(s_{\gamma\gamma},t_{\gamma\gamma}) + D(s_{\gamma\gamma},u_{\gamma\gamma}) + D(u_{\gamma\gamma},t_{\gamma\gamma})] , \quad (7)$$

where $D(s_{\gamma\gamma},t_{\gamma\gamma})$ and $D(s_{\gamma\gamma},u_{\gamma\gamma})$ are the two straight scalar boxes and $D(u_{\gamma\gamma},t_{\gamma\gamma})$ is the crossed scalar box (see, e.g., the second paper in Ref. [6] for the functional form of these scalar integrals in terms of dilogarithms and elementary functions). Here $s_{\gamma\gamma}$, $t_{\gamma\gamma}$, and $u_{\gamma\gamma}$ are the Mandelstam variables for the subprocess $\gamma\gamma \rightarrow ZZ$. This amplitude is concentrated in the forward-backward directions at large energies, and is also logarithmically growing at large energies at fixed scattering angles.

The total cross section is the sum of the contribution from the individual modes. Branching fractions for the subsequent decays of the Z bosons have not been included in the figures or tables. For unpolarized photons there is a factor of one-half from averaging over the initial helicities. In Figs. 3 and 4 the sum of the contributions from all helicity modes is shown for unpolarized photons with an angular cut $|\cos\theta| < 0.9$ on the Z bosons. We emphasize that the angular cut is not particularly effective at reducing the continuum background at $\sqrt{s_{\gamma\gamma}} \approx 300$–$400$ GeV where the background is fairly flat in $\cos\theta$. The angular cut causes the cross section to begin to fall but only mildly in the range $\sqrt{s_{\gamma\gamma}} \gtrsim 700$ GeV, unlike the process $\gamma\gamma \rightarrow W^+W^-$ where a modest cut can reduce the transverse W background by an order of magnitude in the high-energy region [9]. The prominence of the Higgs peak is reduced as the Higgs mass increases; coupled with the rapid raise of the TT background, the viability of $\gamma\gamma \rightarrow H \rightarrow ZZ$ for detecting a heavy Higgs boson deteriorates rapidly with increasing Higgs mass.

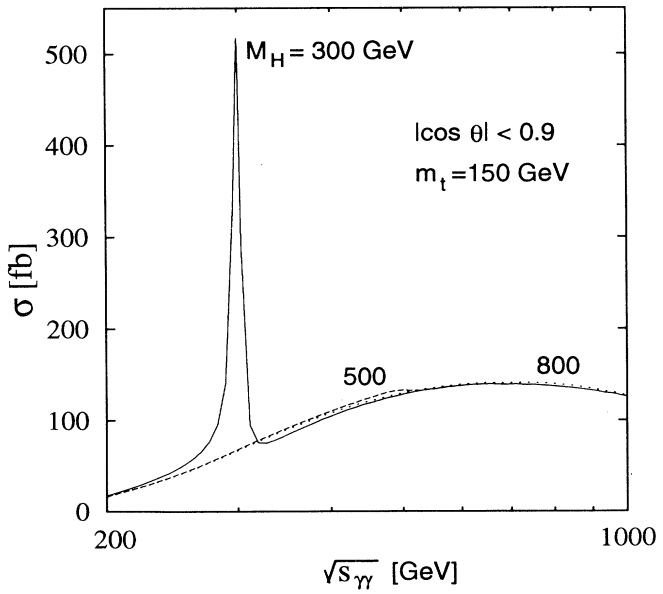

FIG. 3. The total cross section is shown for Higgs-boson masses of 300, 500, and 800 GeV for unpolarized photons after making an angular on the Z bosons of $|\cos\theta| < 0.9$. The top quark mass is taken to be 150 GeV.

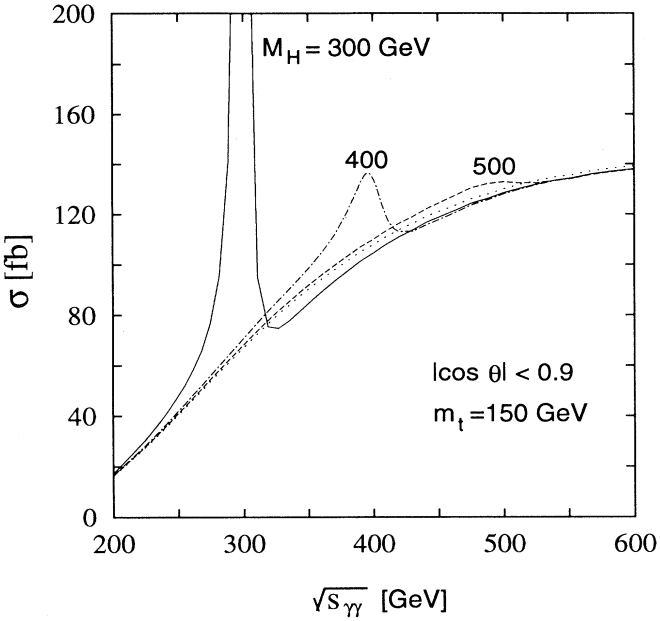

FIG. 4. The total cross section is shown for Higgs-boson masses of 300, 400, and 500 GeV for unpolarized photons after making an angular on the Z bosons of $|\cos\theta| < 0.9$. The dotted line is underlying background. The top quark mass is taken to be 150 GeV.

The peak cross section of the single after subtracting out the underlying background is in close agreement with the form given by the pole approximation:

$$\sigma(\gamma\gamma \rightarrow H \rightarrow ZZ) = \frac{8\pi\Gamma(H \rightarrow \gamma\gamma)\Gamma(H \rightarrow ZZ)}{(s_{\gamma\gamma} - M_H^2)^2 + \Gamma_H^2 M_H^2} , \quad (8)$$

where Γ_H is the total Higgs width. The shape of the signal is changed somewhat due to interference with the underlying continuum background; there is constructive interference below the peak and destructive interference above the peak (see Figs. 2–4). This interference tends to be larger for the Higgs bosons where the signal is less dominant over the background.

One sees from Fig. 4 that as the Higgs-boson mass rises from 300 to 400 GeV, the decreasing prominence of the Higgs peak together with the increasing underlying continuum production of Z's causes the background to become larger than the signal. To obtain event rates one must multiply by the appropriate Z branching fractions and include the photon-photon luminosity distribution. However, one can already deduce that for a Higgs as heavy as 400 GeV, one needs a large number of events since the background is over three times the size of the peak at its maximum.

A brief comment can be made here about the Higgs bosons of extended Higgs sectors and about supersymmetric

Higgs bosons. Extra contributions enter into the loop, e.g., the charged Higgs loops, the squark loops, and chargino loops must be included. These contributions, however, can be deduced from subsets of the calculation already performed in the standard model. This will be the subject of future work. In such cases, we believe this background is still typically large.

III. PHOTON-PHOTON COLLIDERS

The results of the previous section were presented with respect to the invariant mass of the photons. To understand the event rates at a realistic photon-photon collider one must incorporate the spectrum of photons obtained from Compton backscattering a laser beam off the electron beam. We assume the photon beams obtained are unpolarized, thus giving a broad and largely flat luminosity distribution up to approximately 80% of the energy of the e^+e^- collider. We consider three such electron colliders with energies of $E \equiv \sqrt{s_{e^+e^-}} = 500$ GeV, 1 TeV, and 1.5 TeV.

The photon-photon luminosity is given by [10]

$$\frac{dL_{\gamma\gamma}}{dz} = 2\sqrt{\tau} k^2 \int_{\tau/x_m}^{x_m} \frac{dx}{x} F_{\gamma/e}(x,\xi) F_{\gamma/e}(\tau/x,\xi) , \tag{9}$$

where $z^2 = \tau = s_{\gamma\gamma}/s_{e^+e^-}$ and, for unpolarized photons,

$$F_{\gamma/e}(x,\xi) = \frac{1}{D(\xi)} \left[1 - x + \frac{1}{1-x} - \frac{4x}{\xi(1-x)} + \frac{4x^2}{\xi^2(1-x)^2} \right] , \tag{10}$$

$$D(\xi) = \left[1 - \frac{4}{\xi} - \frac{8}{\xi^2} \right] \ln(1+\xi) + \frac{1}{2} + \frac{8}{\xi} - \frac{1}{2(1+\xi)^2} , \tag{11}$$

with the dimensionless parameter

$$\xi = \frac{2\sqrt{s_{e^+e^-}}\,\omega_0}{m_e^2} . \tag{12}$$

We take the conversion coefficient k to be one. The energy of the laser beam cannot be too large, or it would be possible to create electron-positron pairs from an interaction between the laser beam and the backscattered photon. So we take the dimensionless parameter ξ to be 4.82 as usual ($\omega_0 \simeq 1.26$ eV for a 500 GeV e^+e^- collider). The maximum value of the fraction of the incident electron's energy carried by the backscattered photon, x, is then

$$x_m = \frac{\xi}{1+\xi} \approx 0.83 . \tag{13}$$

The luminosity integral in Eq. (9) can be integrated to give an analytic expression [11]:

$$\begin{aligned} \frac{1}{2k^2 z} \frac{dL_{\gamma\gamma}}{dz} = {} & \frac{4}{(1+\xi)\xi^4 D(\xi)^2} [(-4\xi^4 - 4\xi^5 + \xi^6) + (4\xi^2 + 20\xi^3 + 27\xi^4 + 9\xi^5 - 4\xi^6) z^2 \\ & + (-8\xi - 40\xi^2 - 63\xi^3 - 41\xi^4 - 5\xi^5 + 6\xi^6) z^4 + (8 + 32\xi + 54\xi^2 + 48\xi^3 + 21\xi^4 - \xi^5 - 4\xi^6) z^6 \\ & + (-2\xi^2 - 5\xi^3 - 3\xi^4 + \xi^5 + \xi^6) z^8] (-\xi + z^2 + \xi z^2)^{-1} (-1 + z^2)^{-2} \\ & + \frac{1}{\xi^4 D(\xi)^2} [(-8\xi^2 - 8\xi^3 + 2\xi^4) + (40\xi^2 + 20\xi^3 - 6\xi^4) z^2 + (16 - 32\xi - 48\xi^2 - 20\xi^3 + 7\xi^4) z^4 \\ & + (16 + 32\xi + 16\xi^2 + 12\xi^3 - 4\xi^4) z^6 + (-4\xi^3 + \xi^4) z^8] \\ & \times \ln\left[\frac{z^2}{(-\xi + z^2 + \xi z^2)^2} \right] (-1 + z^2)^{-3} + \frac{2}{\xi^2 D(\xi)^2} (4 + 4\xi + \xi^2 + 2\xi z^2) \ln\left[\frac{\xi^2}{(1+\xi)^2 z^2} \right] , \end{aligned} \tag{14}$$

valid in the region $0 < z < x_m$ and equal to zero for $z > x_m$. The cross section is then the convolution of this luminosity with the helicity amplitudes

$$d\sigma = \frac{1}{2} \int_{z^-}^{z^+} dz \frac{dL_{\gamma\gamma}}{dz} \sum_{\lambda_3,\lambda_4} (d\sigma_{++\lambda_3\lambda_4} + d\sigma_{+-\lambda_3\lambda_4}) , \tag{15}$$

where z^- and z^+ are the minimum and maximum of the energy range to be integrated over. To increase the statistical significance of the Higgs peak we integrate over $M_H - \Gamma_H < \sqrt{s_{\gamma\gamma}} < M_H + \Gamma_H$ (we assume that there is sufficient resolution so that $\Gamma_{\rm res} < \Gamma_H$ even for a Higgs as light as 300 GeV) so that

$$z^- = (M_H - \Gamma_H)/\sqrt{s_{e^+e^-}}$$

and

$$z^+ = (M_H + \Gamma_H)/\sqrt{s_{e^+e^-}} .$$

A factor of one half is included to convert these contributions from each helicity mode for unpolarized photon beams because of averaging over the photon helicities. On the other hand, for perfectly polarized photons, one would consider only the modes with equal photon helicities ($++\lambda_3\lambda_4$) yielding an extra factor of 2 in the signal

TABLE I. The cross section for the signal and background (S/B) in the mass range $M_H - \Gamma_H < \sqrt{s_{\gamma\gamma}} < M_H + \Gamma_H$ with no angular cut on the Z bosons.

	$\sqrt{s_{e^+e^-}}$		
M_H	0.5 TeV	1 TeV	1.5 TeV
300 GeV	11.6/3.5	6.7/2.0	4.0/1.2
350 GeV	4.9/8.7	3.1/5.7	2.0/3.6
400 GeV	1.6/8.8	1.4/11.8	0.90/7.7

TABLE III. The cross section for the signal and background (S/B) in the mass range $M_H - \Gamma_H < \sqrt{s_{\gamma\gamma}} < M_H + \Gamma_H$ with the angular cut $|\cos\theta| < 0.8$ on the Z bosons.

	$\sqrt{s_{e^+e^-}}$		
M_H	0.5 TeV	1 TeV	1.5 TeV
300 GeV	9.5/2.6	5.5/1.5	3.3/0.90
350 GeV	4.0/6.2	2.6/4.0	1.6/2.5
400 GeV	1.3/6.1	1.1/8.1	0.74/5.3

[1]. Unfortunately, this also yields a factor 2 in the largest part of the TT background, namely, σ_{++++}. However, we expect some improvement from the unpolarized case since the background σ_{+--+} and σ_{+---+} would be reduced. Another improvement arises from the fact that the polarized photon-photon luminosity can peak more strongly than the unpolarized luminosity.

The cross sections in femtobarns is given in Tables I–IV with the angular cut on the Z's of $|\cos\theta| < 1$, 0.9, 0.8, and 0.7 in the center-of-mass system. Three values of the Higgs mass are considered: $M_H = 300$, 350, and 400 GeV. This range of masses completely covers the region where the Higgs signal is much larger than the continuum background ($M_H = 300$ GeV) to the region where the signal is much smaller than the background ($M_H = 400$ GeV). Both the signal and background for the 400 GeV Higgs is somewhat reduced at the 500 GeV e^+e^- collider, since part of the peak extends past the range of the photon-photon luminosity $z \lesssim 0.83$.

The event rates can be obtained from the figures by incorporating the branching fractions of the Z pairs to some final state. The four-jet decay may be difficult because of the huge $\gamma\gamma \to W^+W^-$ process at the tree level, so one can have one of the Z's decay leptonically. For example, consider the decay mode [3] $ZZ \to q\bar{q}l^+l^-$, $l = e, \mu$ with a branching fraction of 9.5%. With an integrated luminosity of 20 fb^{-1} one has 20 signal events and 5.9 background events for a 300 GeV Higgs at a 500 GeV parent e^+e^- collider employing an angular cut $|\cos\theta| < 0.9$, while one has 8.6 signal events and 14 background events for a 350 GeV Higgs boson. For a 400 GeV Higgs boson the situation is even worse, giving just 2.9 signal events and 14 background events. There are other backgrounds that have been considered [3] in this channel, e.g., $\gamma\gamma \to l^+l^-Z$, $\gamma\gamma \to q\bar{q}Z$, and $\gamma\gamma \to t\bar{t}$ with subsequent decay of the top quarks. Using the results of Ref. [3] we can estimate that the irreducible continuum background is larger than the sum of these backgrounds for $M_H \lesssim 350$ GeV with a reasonable angular cut.

A higher-energy collider will not improve the situation. While the reach of the collider would be greater, less of the photon-photon luminosity would be devoted to the region of the Higgs peak $M_H - \Gamma_H < \sqrt{s_{\gamma\gamma}} < M_H + \Gamma_H$ for the Higgs masses of interest, $M_H < 400$ GeV. For heavier Higgs bosons the continuum background is simply overwhelming.

From the tables it is evident that the angular cut is not effective at eliminating the large TT background. The angular distribution of the TT continuum is rather flat in the range of interest here, $\sqrt{s_{\gamma\gamma}} \approx 300$–40 GeV. For larger $\sqrt{s_{\gamma\gamma}} \gtrsim 1$ TeV the front-back behavior becomes more evident and the angular cut has a more pronounced effect on the cross section (see Fig. 3).

It is possible that the ability to see the Higgs peak above Z_TZ_T background can be improved by employing more refined techniques [1]. Polarized photons have been discussed above. Cuts on the decay products of the Z's can be used to enhance the longitudinal component of the signal over the transverse background. These issues are subject for future study. Since we have obtained the individual helicity amplitudes, we can incorporate the decay density matrices for the Z bosons and recover the full spin correlations of the decay products. In any case, the background is growing very rapidly with energy and it seems unlikely that these methods could change the basic conclusion that the Higgs is unobservable above $M_H = 350$ GeV in its ZZ decay mode.

An interesting corollary to this research is that photon-photon scattering $\gamma\gamma \to \gamma\gamma$ should show the same behavior at very high energies, $\sqrt{s} \gg M_W$. The same helicity amplitudes should eventually grow with energy.

IV. CONCLUSION

We have confirmed the large Z_TZ_T production from photon-photon collisions at high energy. An angular cut

TABLE II. The cross section for the signal and background (S/B) in the mass range $M_H - \Gamma_H < \sqrt{s_{\gamma\gamma}} < M_H + \Gamma_H$ with the angular cut $|\cos\theta| < 0.9$ on the Z bosons.

	$\sqrt{s_{e^+e^-}}$		
M_H	0.5 TeV	1 TeV	1.5 TeV
300 GeV	10.7/3.1	6.1/1.8	3.7/1.1
350 GeV	4.5/7.5	2.9/4.9	1.8/3.1
400 GeV	1.5/7.4	1.3/10.0	0.83/6.5

TABLE IV. The cross section for the signal and background (S/B) in the mass range $M_H - \Gamma_H < \sqrt{s_{\gamma\gamma}} < M_H + \Gamma_H$ with the angular cut $|\cos\theta| < 0.7$ on the Z bosons.

	$\sqrt{s_{e^+e^-}}$		
M_H	0.5 TeV	1 TeV	1.5 TeV
300 GeV	8.3/2.1	4.7/1.2	2.9/0.74
350 GeV	3.5/5.1	2.2/3.3	1.4/2.1
400 GeV	1.1/4.9	1.0/6.4	0.65/4.2

on the Z bosons is ineffective at reducing this background. The search for the heavy Higgs boson should take this background into consideration. The large size of the TT background casts doubt on the viability of the process $\gamma\gamma \to ZZ$ as a "quantum counter" in the high-energy region, since any signal is probably buried beneath the standard model W boson loop contribution. The benefits of polarized photon beams and cuts on the decay products of the Z bosons in detecting a heavy Higgs boson including the continuum background considered here is a subject for future study.

Note added in proof. Jikia [12] has recently published the helicity amplitudes for the process $\gamma\gamma \to ZZ$. We have performed a detailed check of Eqs. (3-6) through (3-23) of Ref. [12], and find complete agreement apart from one term in the amplitude A_{+-+0} which should be replaced as follows: $-24c_W^2 m_W^2 u_1 \to -24c_W^2 m_W^2 u_1 / s s_4$. Two other recent calculations [13,14] of $\gamma\gamma \to ZZ$ also find numerical agreement.

ACKNOWLEDGMENTS

We wish to thank V. Barger, G. Bhattacharya, D. Bowser-Chao, M. Chanowitz, K. Cheung, A. Djouadi, and C. Kao for useful discussions. This research was supported in part by the University of Wisconsin Research Committee with funds granted by the Wisconsin Alumni Research Foundation, in part by the U.S. Department of Energy under Contract No. DE-AC02-76ER00881, and in part by the Texas National Laboratory Research Commission under Grant No. RGFY 93-221.

[1] J. F. Gunion and H. E. Haber, in *Research Directions for the Decade,* Proceedings of the Summer Study on High Energy Physics, Snowmass, Colorado, 1990, edited by E. L. Berger (World Scientific, Singapore, 1991); J. F. Gunion and H. E. Haber, University of California Report No. UCD-92-22, 1992 (unpublished); J. F. Gunion, this issue, Phys. Rev. D **48**, 5109 (1993).

[2] D. L. Borden, D. A. Bauer, and D. O. Caldwell, SLAC Report No. SLAC-PUB-5715, 1992 (unpublished).

[3] K. Cheung and D. Bowser-Chao, Phys. Rev. D **48**, 89 (1993); K. Cheung, talk given at the "Workshop on Physics and Experiments with Linear e^+e^- Collider" (unpublished)

[4] M. Chanowitz, Phys. Rev. Lett. **69**, 2037 (1992).

[5] G. V. Jikia, Phys. Lett. B **298**, 224 (1993).

[6] E. W. N. Glover and J. J. van der Bij, Phys. Lett. B **219**, 488 (1989); Nucl. Phys. **B321**, 561 (1989). See also D. A. Dicus, C. Kao, and W. W. Repko, Phys. Rev. D **36**, 1570 (1987); D. A. Dicus, *ibid.* **38**, 394 (1988).

[7] G. J. van Oldenborgh and J. A. M. Vermaseren, Z. Phys. C **46**, 425 (1990).

[8] O. P. Sushkov, V. V. Flambaum, and I. B. Khriplovich, Yad. Fiz. **20**, 1016 (1975) [Sov. J. Nucl. Phys. **20**, 537 (1975)]; I. F. Ginzburg, G. L. Kotkin, S. L. Panfil, and V. G. Serbo, Nucl. Phys. **B228**, 285 (1983).

[9] See, e.g., G. Bélanger and E. Boudjema, Phys. Lett. B **228**, 210 (1992), and references therein.

[10] I. F. Ginzburg, G. L. Kotkin, V. G. Serbo, and V. I. Telnov, Nucl. Instrum. Methods **205**, 47 (1983); **219**, 5 (1984); V. I. Telnov, Nucl. Instrum. Methods A **294**, 72 (1990); O. J. P. Eboli, M. C. Gonzalez-Garcia, F. Halzen, and S. F. Novaes, Phys. Rev. D **47**, 1889 (1993).

[11] It is interesting to note that the luminosity in Eq. (9) can be performed analytically even for polarized beams.

[12] G. V. Jikia, Nucl. Phys. **B405**, 24 (1993).

[13] B. Bajc, Phys. Rev. D **48**, R1907 (1993).

[14] D. A. Dicus and C. Kao, Florida State University Report No. FSU-HEP-930808, 1993 (unpublished).